ChemSystemsChem

Research Article
doi.org/10.1002/syst.202500025

Chemistry Europe
European Chemical Societies Publishing

www.chemsystemschem.org

# Emergence and Competing Selectivity of Minimal Self-Assembly Lipoamino Acids

Luis Calahorra-Rio[a, b] and Ignacio Colomer*[a]

*Ignacio Colomer has been nominated for the special collection Systems Chemistry Talents by Board Member Javier Montenegro*

Designing synthetic chemical systems capable of mimicking life-like behavior surely will help to understand the basic principles sustaining life, but also to create advanced materials potentially going beyond nature. Herein, we report the synthesis of a family of lipoamino acids from their individual components, which are free amino acids and lipid precursors, that allow us to study competition and selection in their formation. Octanoyl-*L*-histidine outcompetes from a pool of natural amino acids and a family of lipids, emerging as the fittest, where the observed selectivity is the result of a very efficient autocatalytic mechanism.

## 1. Introduction

Lipoamino acids are amphiphilic molecules in which a hydrophobic aliphatic chain is attached to either the carboxylic group (via a fatty amine or alcohol) or the amino group (via a fatty alkyl or acyl moiety).[1,2] The amphiphilic character of lipoamino acids and the structural motifs, primarily the amino acid side chain and the length and substitution of the lipid, determine their self-assembly. However, lipoamino acids show a very rich and diverse supramolecular morphology, including micelles, vesicles, fibers, twisted ribbons, or tubules, with interesting stimuli-responsive properties, influenced by concentration, time, solvent, pH, or additive effects. In this sense, both natural and synthetic lipoamino acids have shown important applications across many different areas, for example, in water purification and industrial oil recovery, as antibiotics, antitumoral, or neuroprotective agents, or in drug delivery (Figure 1A).[3,4] The ability of lipoamino acids to catalyze certain reactions, such as ester hydrolysis, and their parallelism as minimal mimetics of enzymes has invigorated the design of bioinspired members with outstanding catalytic properties (Figure 1A).[5] In addition, histidine-based lipoamino acids have been recently used to design synthetic systems with life-like properties, showing catalytic activity under a non-equilibrium regimen (Figure 1A).[6]

In connection with exploring other life-like phenomena using synthetic chemical systems, natural selection processes emerge as a fundamental mechanism that living systems incorporate into the inexorable natural evolution. However, how to translate the idea of competition for a limited resource and selection for the fittest members to ultimately achieve chemical evolution at a molecular and supramolecular level is something that we still do not understand completely.[7–9] This is a challenging topic that has only been approached recently with only a few contributions, that we can group in (Figure 1B): 1) lipid replicators whose precursors compete between them, using alkene metathesis, azide–alkyne cycloaddition or thiol–disulfide exchange reactions;[10–12] 2) fatty anhydrides generated as out-of-equilibrium species from their corresponding fatty acids, where the selection is based on the phase-separation (i.e., droplets) of a given member;[13,14] 3) selection in the formation of competing phospholipids, based on their differentiated stability toward hydrolysis;[15] 4) template nucleopeptide replicators formed from their precursors, where selection is observed when seeding with a given nucleopeptide replicator;[16,17] 5) self-replicators formed from a dynamic combinatorial library showing selection based on their differentiated kinetic properties;[18] 6) selection in peptide synthesis using aminoacyl phosphate esters based on side chain interactions.[19] Moreover, efforts to combine a compartmentalized system encapsulating an autocatalytic reaction showing growth and division or competition and selection phenomena have recently been reported.[20]

Herein, we aim at using a collection of lipoamino acids, generated in situ from their hydrophilic and hydrophobic components, with differentiated chemical and supramolecular properties, that can compete and potentially show selection in their synthesis and emergence (Figure 1C).

## 2. Results and Discussion

We began our study screening a selection of representative amino acids with diverse properties, including hydrophobic aliphatic (valine, **Val**) and aromatic (phenylalanine, **Phe**), hydrophilic neutral (serine, **Ser**), acid (glutamic acid, **Glu**), and basic (lysine, **Lys**; arginine, **Arg** and histidine, **His**) side chains. Based on our previous experience in self-assembly lipoamino

[a] *L. Calahorra-Rio, Dr. I. Colomer*
*Instituto de Química Orgánica General (IQOG-CSIC), Juan de la Cierva 3, Madrid 28006, Spain*
*E-mail: colomer@iqog.csic.es*

[b] *L. Calahorra-Rio*
*IMDEA Nanociencia, Faraday 9, Madrid 28049, Spain*

*Supporting information for this article is available on the WWW under https://doi.org/10.1002/syst.202500025*

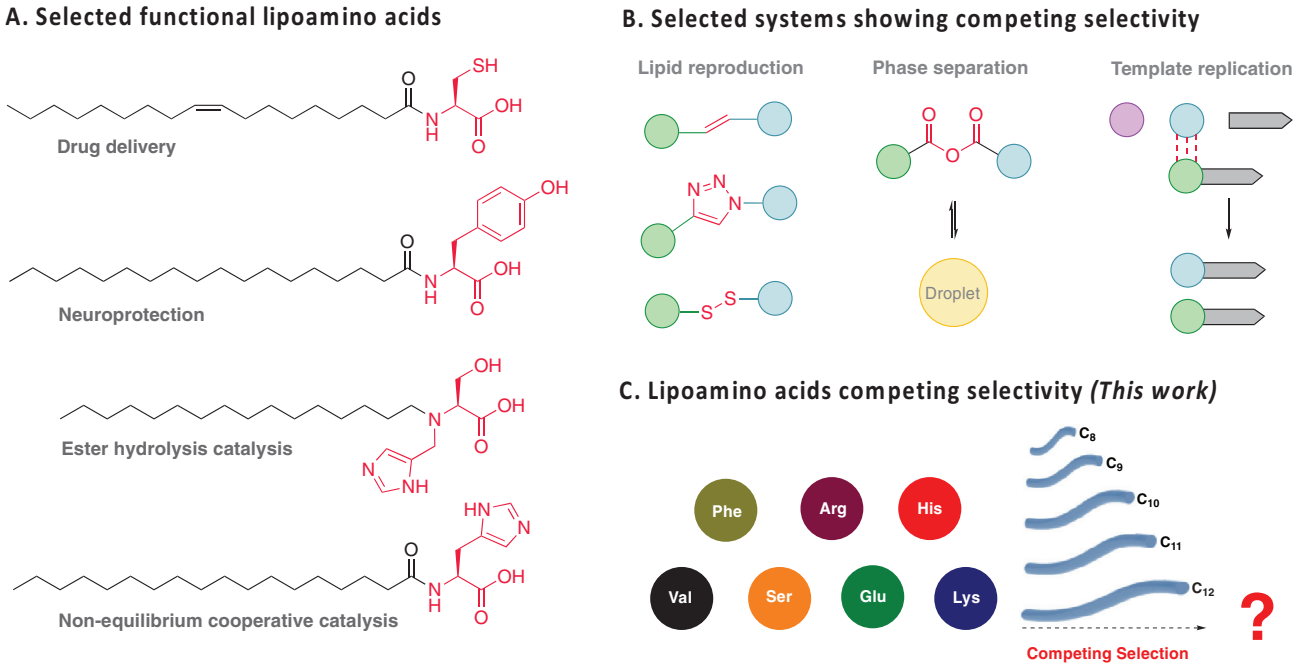


**Figure 1.** A) Lipoamino acids showing biomedical application and biological or catalytic activities. B) Previous strategies showing competing selectivity include lipid and template replicators. C) This work studies competing selectivity within lipoamino acids synthesis.

acids,[21] after a first preliminary screening, we considered using fatty acyl chlorides as hydrophobic precursors under phase-separated conditions, which would minimize the acyl chloride hydrolysis.

Using a solution of the corresponding amino acid (**aa**) and $Na_2CO_3$ in water and Octanoyl chloride (**$C_8$-Cl**) in heptane, we were able to observe the formation of the corresponding amphiphilic species *N*-Octanoyl amino acid (**$C_8$-aa**). While **Val**, **Ser**, **Lys**, and **Glu** give traces of product or low isolated yields, **Phe**, **Arg,** and **His** afford the desired products in good to excellent isolated yields, the latter arising the best outcome. The exceptionally good result of **His** could be related to the acyl transfer capacity of imidazole, within the side chain of **His**, that might help the acylation reaction across the interface (Figure 2).[22,23] Thus, we opted to continue selecting **His** as the optimal model amino acid, evaluating lipid chains of different lengths. Longer fatty acyl chlorides were effective, and the corresponding **$C_9$-His**, **$C_{10}$-His**, **$C_{11}$-His,** and **$C_{12}$-His** could be isolated in moderate yields (Figure 2). Nonetheless, shorter lipid chains either do not provide self-assembly species or are not highly competent in the reaction (**$C_5$-His**, **$C_6$-His**, or **$C_7$-His**), presumably because the acyl chlorides partition in the water phase and are rapidly hydrolyzed (Figure 2). This is a neat example of the key role of phase-separation, protecting the fatty acyl reagents.

At this point, we chose **$C_8$-His** as a model system to investigate both its supramolecular properties and the kinetic behavior of the transformation (Figure 3A). We carried on the supramolecular characterization of **$C_8$-His**, first determining the critical aggregation concentration (CAC), using an established spectrofluorimetric method measuring the emission of fluorophore rhodamine 6G,[24] that arose a value of 7.86 mM (Figure 3B). As it is expected, longer hydrophobic chains have lower values of CAC, while shortening them shows much higher CAC or no aggregation (see Supporting Information for a complete study). Dynamic Light Scattering (DLS) was used to evaluate the size of **$C_8$-His** assemblies across the pH scale, where a population of 20–60 nm is detected between pH 7–12, at which the carboxylate might be present, correlating with stable nanoparticles and a Zeta-potential (ZP) value of −20 mV, confirming the overall negative charge within the nanoparticle surface (Figure 3C). At lower pH, between 3–7, larger polydisperse aggregates are detected together with a decrease in the stability and ZP values approaching 0, probably due to imidazole protonation and no global charge ($pK_2 = 7.07$ for **$C_2$-His**).[25] Highly acidic pH, below 3, shows particles under 100 nm and slightly positive ZP values, which would match with carboxylic acid species and a positive net charge ($pK_1 = 3.08$ for **$C_2$-His**).[25] Finally, the morphology of these nanoparticles was studied using transmission electron microscopy (TEM) under uranyl acetate negative staining, showing micelles with an average size of 30 nm in samples of **$C_8$-His** at 10 mM concentration (Figure 3D and Supporting Information).

The kinetic analysis of both **His** consumption and **$C_8$-His** formation was performed by extracting aliquots of the reaction mixture to determine the concentration of both species using HPLC-DAD (see Supporting Information for further chromatographic details and stacked chromatograms). They show a sigmoidal curve with a 1 h lag period that is followed by an exponential rate increase to complete the transformation in a 4 h period and non-linear kinetics (Figure 3E). It is important to emphasize that a similar kinetic behavior is observed for different longer fatty acyl chlorides using **His** (see Supporting Information for the complete study). This effect and the lag period are suppressed when the experiment is seeded from the beginning with the product of the reaction, **$C_8$-His**, in a concentration above the CAC, where micellar self-assembly is present from the beginning. Thus, adding 15 mol% of **$C_8$-His** (25 mM),

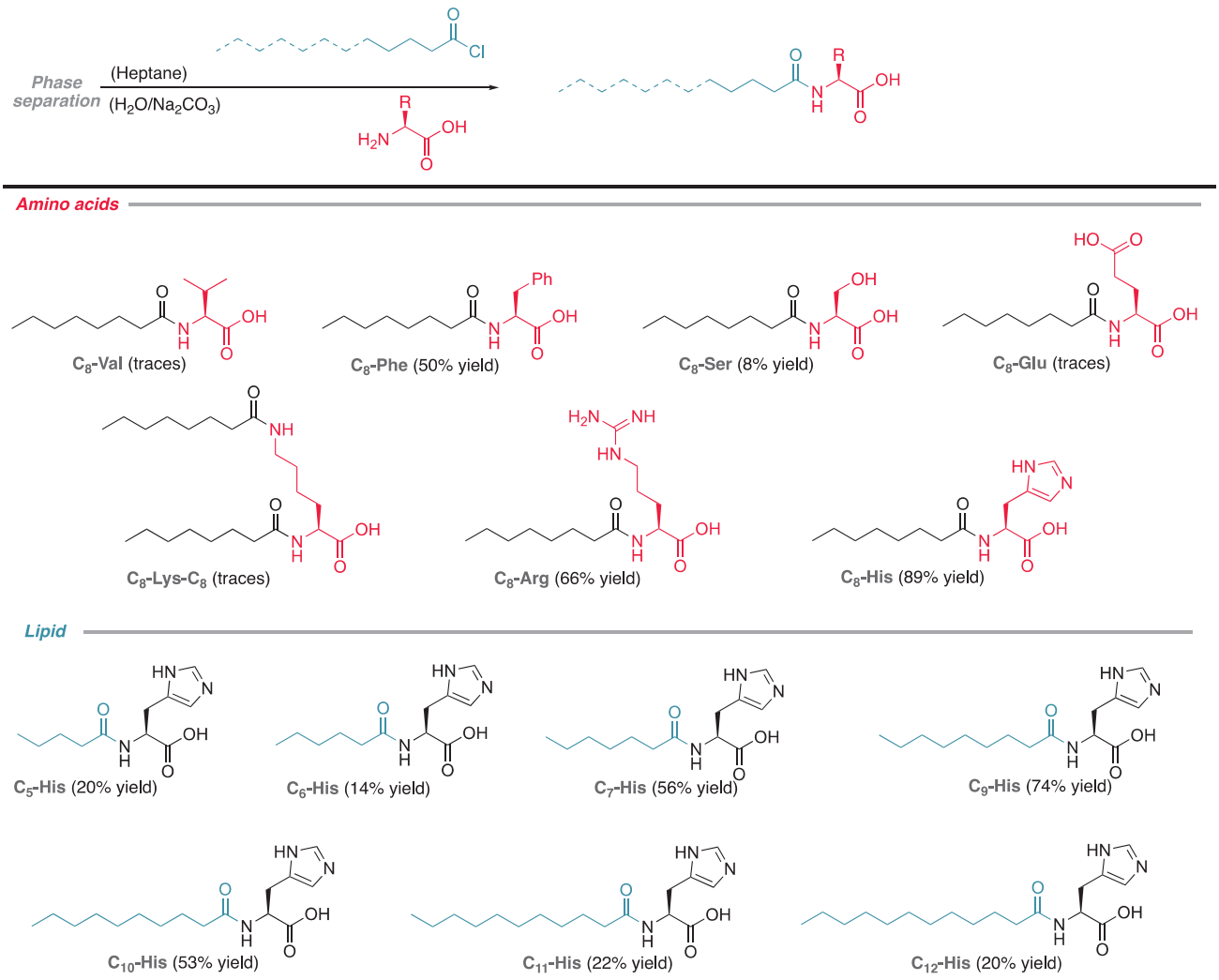


**Figure 2.** Screening of amino acids and acyl chlorides for the synthesis of minimal self-assembly lipoamino acids. Standard conditions: amino acid (1.0 equiv) and $Na_2CO_3$ (2.0 equiv) in Milli-Q water, and acyl chloride (6.0 equiv) in heptane, stirred at 330 rpm and RT.

the transformation is completed in 1 h (Figure 3F and Supporting Information for further details and the effect of other catalyst loadings). Taken all together, these experiments support an autocatalytic behavior,[26] where the micellar self-assembly product **$C_8$-His** catalyzes the formation of its amphiphilic monomers via phase transfer catalysis. It is important to emphasize that phase separation is key to achieve a productive transformation; otherwise, using one-phase conditions (THF/$H_2O$), no autocatalysis and less than 30% conversion are observed (see Supporting Information for further details). A related strategy showing an autocatalytic mechanism using short peptides and lipid precursors via an imine formation has been recently reported.[27]

With this robust self-reproductive amino acid lipidation in hand, we were intrigued to explore further more complex phenomena, such as competition and selection, that could be studied following two complementary approaches: 1) different acyl chlorides that compete for a single amino acid as a limiting resource, or 2) different amino acids that compete for a single limiting acyl chloride.

Initially, we investigated the first option, using **His** as the sole amino acid and a 1:1 mixture of octanoyl chloride and dodecanoyl chloride (the shortest and longest lipids that promote efficient self-assembly as previously shown), under standard conditions (Figure 4A). The kinetic analysis of both **His** consumption and **$C_8$-His** formation resembles that in Figure 3E, following a sigmoidal curve with an initial induction period that is followed by an exponential growth in the formation of **$C_8$-His** as a sole product during the first 3 h, reaching a maximum up to 125 mM (85% conversion of **His**, Figure 4B). Only when the concentration of **$C_8$-His** has surpassed the CAC to self-assemble into micelles and the reaction is within the exponential regimen, we observed the appearance of **$C_{12}$-His**, reaching a maximum of 25 mM (15% conversion of **His**, Figure 4B). Thus, **$C_8$-His** is produced in a concentration almost six times higher than **$C_{12}$-His**, showing a high preference for lipoamino acid **$C_8$-His**. Moreover, the formation of **$C_{12}$-His** seems to correlate with the micellar phase transfer ability of **$C_8$-His** to cross-catalyze its formation.

Pushing the boundaries of the system, we designed a challenging experiment where all acyl chlorides promoting self-assembly (**$C_8$**, **$C_9$**, **$C_{10}$**, **$C_{11}$**, and **$C_{12}$**) were put together in an equimolecular mixture, so that up to five different self-assembly lipoamino acids could be formed, just differing in one methy-

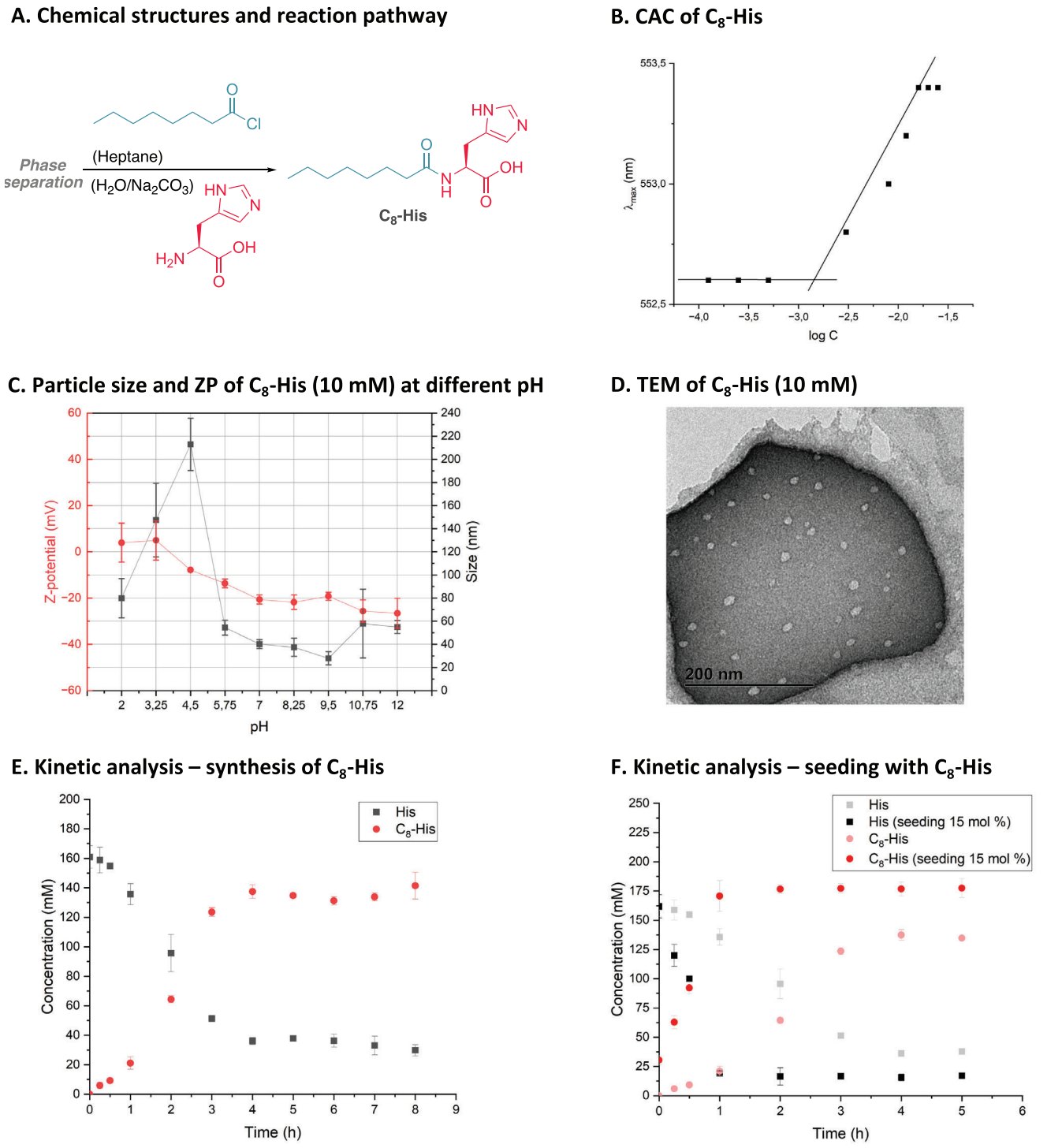


**Figure 3.** Supramolecular characterization and kinetic analysis for the synthesis of lipoamino acid **$C_8$-His**. A) Model reaction. B) Critical Aggregation Concentration (CAC) calculated using rhodamine 6G emission. C) Particle size and Z-potential (ZP) using dynamic light scattering (DLS). D) Transmission electron microscopy (TEM) showing micelles. E) Kinetic analysis for the synthesis of **$C_8$-His** under standard conditions. F) Kinetic analysis for the synthesis of **$C_8$-His,** seeding the experiment with 15 mol% of product **$C_8$-His** (25 mM).

lene unit to each other. The kinetic analysis reveals a similar trend with **$C_8$-His** being exclusively formed during the first hour and a peaking concentration of 65 mM (45% conversion of **His**, Figure 4C). The rest of lipoamino acids only start forming when **$C_8$-His** has surpassed the CAC and is reaching its maximum, and show peaking concentrations of 24 mM for **$C_9$-His** (16% conversion of **His**, Figure 4C), 21 mM for **$C_{10}$-His** (14% conversion of **His**, Figure 4C), 12 mM for **$C_{11}$-His** (8% conversion of **His**, Figure 4C), and 20 mM for **$C_{12}$-His** (13% conversion of **His**, Figure 4C). Again, the selectivity toward **$C_8$-His** is excellent with a selective factor of almost 6 with respect to **$C_{11}$-His** and almost 3 with respect to **$C_9$-His**, **$C_{10}$-His**, and **$C_{12}$-His** (Figure 4D). For this experiment, plot-

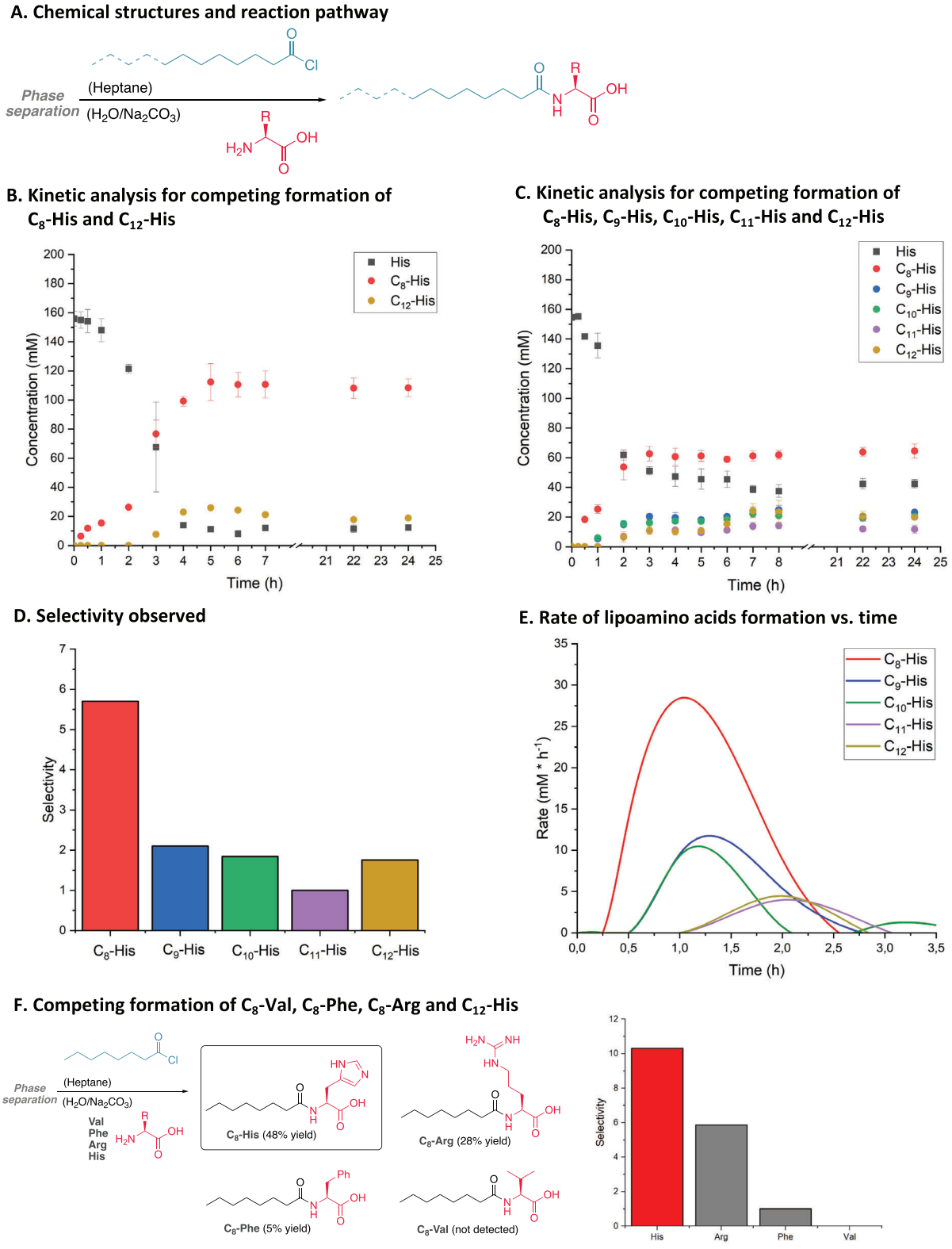


**Figure 4.** Competing selectivity of self-assembly lipoamino acids. A) Model reaction. B,C) Mixtures of acyl chlorides compete for a single amino acid (**His**). D) Selectivity toward **$C_8$-His** is observed. E) Rate of formation could explain the selectivity toward **$C_8$-His**. F) Mixture of amino acids compete for a single acyl chloride (octanoyl chloride), showing selectivity toward **$C_8$-His** formation.

ting the rate of formation for every lipoamino acid within the first 3 h, when the reaction is completed, helps to understand the high selectivity towards **$C_8$-His** in the competing experiments. First, the peaking rates of formation follow the trend: **$C_8$-His** (28 mM/h, Figure 4E), **$C_9$-His**, and **$C_{10}$-His** (11 and 10 mM/h, Figure 4E), **$C_{11}$-His,** and **$C_{12}$-His** (5 mM/h, Figure 4E). Second, the moment of the peaking rate (related to the induction period) follows a similar trend: **$C_8$-His** (after 1 h, Figure 4E), **$C_9$-His** and **$C_{10}$-His** (after 1.5 h, Figure 4E), **$C_{11}$-His** and **$C_{12}$-His** (after 2 h, Figure 4E). Therefore, a faster kinetics, determined by a higher rate of formation and a shorter induction period within the autocatalytic reaction, is the origin of the high competing selectivity towards lipoamino acid **$C_8$-His**. Once again, the phase separation is key to achieve the observed selectivity; otherwise, using one-phase conditions (THF/$H_2O$), conversion and/or selection were negligible (see Supporting Information for further details).

Finally, we took on the challenge of studying the complementary competing experiment, where a mixture of amino acids would compete for a sole acyl chloride (**$C_8$-Cl**). Without biasing the system, we opted to use those amino acids performing better in the initial screening (Figure 2). Thus, using an equimolecular mixture of **Val**, **Phe**, **Arg**, and **His** under standard conditions and octanoyl chloride as the lipid precursor, the analysis of the reaction outcome revealed a high selectivity toward **$C_8$-His** (48% yield) with respect to **$C_8$-Arg** (28% yield) and **$C_8$-Phe** (5% yield), while **$C_8$-Val** is not detected (Figure 4F). These results confirm the exceptional ability of **$C_8$-His** to emerge as the fittest member of the population.

## 3. Conclusion

In summary, we have developed a new system based on the synthesis and self-assembly of amphiphilic lipoamino acids from their individual components, which are free amino acids and fatty acyl chlorides, under phase-separated conditions. The process follows an autocatalytic mechanism, where the lipoamino acid micellar self-assembly catalyzes the formation of its amphiphilic monomers. This system has allowed us to study challenging and relevant phenomena that go beyond the molecular behavior, such as competition and selection. Following two approaches, either a sole amino acid competing for a family of lipid precursors or a group of amino acids competing for a sole lipid, in both cases, octanoyl-*L*-histidine, **$C_8$-His**, has emerged as a minimal lipoamino acid that outcompetes as the preferred self-assembly product. We are currently exploring the use of these lipoamino acids in more complex behaviors, controlling their spatiotemporal existence, as self-assembly catalysts or in controlled delivery.

## 4. Experimental Methods

### 4.1. Synthesis of Lipoamino Acids under Phase-Separation

In a 25 mL round bottom flask, to a solution of the corresponding free amino acid (0.64 mmol, 1.0 equiv) and $Na_2CO_3$ (1.28 mmol, 2.0 equiv) in 4.0 mL of Milli-Q water, was carefully added a solution of the corresponding acyl chloride (3.84 mmol, 6.0 equiv) in 4.0 mL of heptane, keeping the phase separation and avoiding both phases to mix. The reaction was stirred at 330 rpm and RT until completion. Both phases are separated; the aqueous phase is neutralized using HCl (6.0 M), extracted with EtOAc (three times), washed with brine, and dried over anhydrous $Na_2SO_4$. The organic solvent was removed, and the crude reaction was purified by column chromatography (gradient elution: 0:100 → 30:70 $CH_2Cl_2$–MeOH).

### 4.2. Kinetic Analysis

The reactions were monitored by extracting an aliquot of 5 µL of the aqueous phase at every selected time, which was diluted up to a total volume of 0.3 mL with a stock standard solution of 1.0 mM of phenol in $H_2O$, using an Agilent Technologies 1200 Series HPLC system with a diode array detector (DAD). Phoroshell 120 EC-C18 column 4.6×150 mm with 4 µm size particle was used as a stationary phase, and a mixture of $H_2O$ (0.1% TFA) : MeOH (0.1% TFA) with a gradient of 100:0 to 0:100 over 20 min at a fixed temperature (37.5 °C) as mobile phase.

### 4.3. Critical Aggregation Concentration (CAC)

Basic aqueous solutions (pH = 8.5, Bicine) of the corresponding lipoamino acid were prepared, containing rhodamine 6G (1 µM), with a surfactant lipoamino acid concentration ranging from 25 to 0.125 mM. Analyses were performed using a Cary Eclipse Varian spectrofluorometer, with an excitation wavelength of 520 nm and the emission wavelength switched from 552 to 560 nm. CAC values were obtained by plotting the maximum wavelength of emission ($\lambda$ max/nm) against the logarithm of the surfactant concentration (C/mM).

### 4.4. Particle size and Z-Potential using Dynamic Light Scattering (DLS)

Disposable folded capillary cuvettes were filled with 1.0 mL of a 10 mM sample solution, previously filtrated through 0.22 µm nylon syringe filters, equilibrating the samples at 25 °C for 25 s before particle size and ZP measurements, using a Malvern Zetasizer PRO equipment.

### 4.5. Transmission Electron Microscopy (TEM)

10 mM samples of lipoamino acids in Milli-Q water are prepared and filtered through a 0.22 µm nylon filter. One drop of the sample is poured carefully on the coated surface of the grid for 2 min. After drying and removing the excess, grids are negative stained using uranyl acetate solution (1% m/V). After 30 s, the excess of the staining solution is removed, the grids are dried again, and processed in a JEOL JEM 1400 with working voltage from 40 to 120 KV.

## Acknowledgments

The authors acknowledge funding from the Spanish MICIU/AEI/10.13039/501100011033 (grants PID2019-106327GA-I00 and PID2022-141911NB-I00 to I.C. and predoctoral fellowship PRE2020-095493 to L.C.) and CSIC (PIE 20218AT015 and PIE 202280I025).

## Conflict of Interests

The authors declare no conflict of interest

## Data Availability Statement

The data that support the findings of this study are available in the supplementary material of this article.

**Keywords:** Acylation · Amino acid · Autocatalysis · Lipids · Selectivity

[1] R. Bordes, K. Holmberg, *Adv. Colloid Interface Sci.* **2015**, *222*, 79–91.
[2] K. Holmberg, F. Bilén, R. Bordes, *Curr. Opin. Colloid Interface Sci.* **2025**, *75*, 101884.
[3] X. Du, J. Zhou, J. Shi, B. Xu, *Chem. Rev.* **2015**, *115*, 13165–13307.
[4] C. Vicente-Garcia, I. Colomer, *Nat. Rev. Chem.* **2023**, *7*, 710–731.
[5] M. D. Nothling, Z. Xiao, N. S. Hill, M. T. Blyth, A. Bhaskaran, M.-A. Sani, A. Espinosa-Gomez, K. Ngov, J. White, T. Buscher, F. Separovic, M. L. O'Mara, M. L. Coote, L. A. Connal, *Sci. Adv.* **2020**, *6*, eaaz0404.
[6] S. Bal, K. Das, S. Ahmed, D. Das, *Angew. Chem. Int. Ed.* **2019**, *58*, 244–247.
[7] G. Danger, L. L. S. d'Hendecourt, R. Pascal, *Nat. Rev. Chem.* **2020**, *4*, 102–109.
[8] A. Kahana, D. Lancet, *Nat. Rev. Chem.* **2021**, *5*, 870–878.
[9] M. G. Howlett, S. P. Fletcher, *Nat. Rev. Chem.* **2023**, *7*, 673–691.
[10] I. Colomer, A. Borissov, S. P. Fletcher, *Nat. Commun.* **2020**, *11*, 176.
[11] E. A. J. Post, S. P. Fletcher, *Chem. Sci.* **2020**, *11*, 9434–9442.
[12] M. G. Howlett, R. J. H. Scanes, S. P. Fletcher, *JACS Au* **2021**, *1*, 1355–1361.
[13] M. Tena-Solsona, C. Wanzke, B. Riess, A. R. Bausch, J. Boekhoven, *Nat. Commun.* **2018**, *9*, 2044.
[14] P. S. Schwarz, S. Laha, J. Janssen, T. Huss, J. Boekhoven, C. A. Weber, *Chem. Sci.* **2021**, *12*, 7554–7560.
[15] C. Bonfio, C. Caumes, C. D. Duffy, B. H. Patel, C. Percivalle, M. Tsanakopoulou, J. D. Sutherland, *J. Am. Chem. Soc.* **2019**, *141*, 3934–3939.
[16] A. K. Bandela, N. Wagner, H. Sadihov, S. Morales-Reina, A. Chotera-Ouda, K. Basu, R. Cohen-Luria, A. de la Escosura, G. Ashkenasy, *Proc. Natl. Acad. Sci* **2021**, *118*, e2015285118.
[17] S. Vela-Gallego, Z. Pardo-Botero, C. Moya, A. de la Escosura, *Chem. Sci.* **2022**, *13*, 10715–10724.
[18] B. Liu, J. Wu, M. Geerts, O. Markovitch, C. G. Pappas, K. Liu, S. Otto, *Angew. Chem. Int. Ed.* **2022**, *61*, e202117605.
[19] A. Sharma, K. Dai, M. D. Pol, R. Thomann, Y. Thomann, S. K. Roy, C. G. Pappas, *Nat. Commun.* **2025**, *16*, 1306.
[20] H. Lu, A. Blokhuis, R. Turk-MacLeod, J. Karuppusamy, A. Franconi, G. Woronoff, C. Jeancolas, A. Abrishamkar, E. Loire, F. Ferrage, P. Pelupessy, L. Jullien, E. Szathmary, P. Nghe, A. D. Griffiths, *Nat. Chem.* **2024**, *16*, 70–78.
[21] C. Vicente-García, I. Colomer, *Org. Biomol. Chem.* **2021**, *19*, 6797–6803.
[22] W. P. Jencks, J. Carriuolo, *J. Biol. Chem.* **1959**, *234*, 1280–1285.
[23] K.-J. Huang, Y.-C. Huang, Y. A. Lin, *Chem. Asian J.* **2018**, *13*, 400–403.
[24] I. Abdalla, J. Xu, D. Wang, H. Tong, B. Sun, B. Ding, X. Jiang, M. Zhu, *RSC Adv.* **2019**, *9*, 1814–1821.
[25] M. Tanokura, M. Tasumi, T. Miyazawa, *Biopolymers* **1976**, *15*, 393–401.
[26] A. J. Bissette, S. P. Fletcher, *Angew. Chem. Int. Ed.* **2013**, *52*, 12800–12826.
[27] I. Turcan, I. Insua, *ChemSystemsChem* **2025**, *7*, e202400094.

Manuscript received: May 14, 2025
Revised manuscript received: July 21, 2025
Version of record online: August 14, 2025